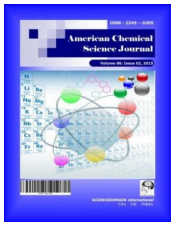

*American Chemical Science Journal*
*15(4): 1-11, 2016, Article no.ACSJ.28010*
*ISSN: 2249-0205*

**SCIENCEDOMAIN** *international*
www.sciencedomain.org

# Synthesis and Characterization of Lanthanum Strontium Cobalt Ferrite Nanoparticles Prepared by Thermal Decomposition of the Mixed Metal Acetylacetonates

**Julius Numbonui Ghogomu[1*], Edwin Akongnwi Nforna[1] and John Ngolui Lambi[2]**

*[1]Department of Chemistry, University of Dschang, P.O.Box 67, Dschang, WR, Cameroon.*
*[2]Department of Chemistry, Higher Teacher's Training College Yaounde, University of Yaoundé I, P.O.Box 47 Yaoundé, CR, Cameroon.*

***Authors' contributions***

*This work was carried out in collaboration with all the authors. Author JNG designed the protocol, participated in writing the first draft of the manuscript and provided the literature review. Author EAN performed the experiments and wrote the first draft of the manuscript. Author JNL designed the work, managed the interpretation of results as well as proof reading the work. All authors read and approved the final manuscript.*

***Article Information***

DOI: 10.9734/ACSJ/2016/28010
Editor(s):
(1) Francisco Marquez-Linares, Full Professor of Chemistry, Nanomaterials Research Group School of Science and Technology, University of Turabo, USA.
Reviewers:
(1) Volodymyr Krasnoholovets, Institute of Physics, Natl. Acad. Sci, Ukraine.
(2) R. S. Rimal Isaac, Noorul Islam Centre for Higher Education, India.
Complete Peer review History: http://www.sciencedomain.org/review-history/15612

***Original Research Article***

***Received 29th June 2016***
***Accepted 21st July 2016***
***Published 31st July 2016***

## ABSTRACT

**Aims:** To synthesis lanthanum strontium cobalt ferrite, $La_{0.8}Sr_{0.2}Co_yFe_{1-y}O_{3-\delta}$ (y=0, 0.2, 0.4) nanopowders via metal-organic precursors (acetylacetonates), determine the composition, structure and magnetic properties.
**Place and Duration of Study:** Laboratory of Noxious Chemistry and Environmental Engineering – University of Dschang and Magnetic Materials Unit, National Chemical Laboratory, Pune – India between November 2013 and March 2015.
**Methodology:** Mixed lanthanum strontium cobalt iron acetylacetonate precursors were synthesized

**Corresponding author: E-mail: ghogsjuju@hotmail.com;*

at 55°C by co-precipitation and heated at 450°C to undergo thermal decomposition in order to form mixed lanthanum strontium cobalt ferrite alongside secondary phases. They were further calcined at 1000°C to form single perovskite phase. The structure, morphology and elemental analyses were determined by X-ray diffraction, scanning electron microscopy and energy dispersive X-ray spectroscopy respectively. The magnetic properties were determined at room temperature using a vibrating sample magnetometer.

**Results:** X-ray diffraction studies of heat-treated $La_{0.8}Sr_{0.2}Co_yFe_{1-y}O_{3-\delta}$ showed that single phase nano-sized perovskite powders were formed with structures varying from orthorhombic (y = 0, 0.2) to rhombohedral (y =0.4) as the Co content increased. Microstructure analysis indicated polycrystalline spherical nanoparticles with agglomeration tendencies. Elemental analysis by X-ray energy dispersive spectroscopy indicated that the desired metals in their stoichiometric proportions were obtained. From the measured hysteresis loops of $La_{0.8}Sr_{0.2}Co_yFe_{1-y}O_3$ at room temperature using a vibrating sample magnetometer, all the compositions exhibited anti ferromagnetism and a weak ferromagnetic component along the c-axis as a result of the complex interaction of different valences of the transition metal ions. Increasing coercive fields were observed with increasing Co content while spontaneous magnetization and saturation magnetization decreased with increased in Co substitution.

**Conclusion:** $La_{0.8}Sr_{0.2}Co_yFe_{1-y}O_3$ was successfully prepared by the thermal decomposition method. Their structural and magnetic properties were found to vary with the Co content. These results show that the synthesized materials possess potential magnetic applications in data storage, logic, magnetic bubble memory, magnetic sensors.

*Keywords: Lanthanum strontium cobalt ferrite nanoparticles; perovskite; x-ray diffraction; ferromagnetism; anti ferromagnetism.*

## 1. INTRODUCTION

Rapid technological advances demand for the search of novel materials with special properties for specific applications. One important class of such compounds with wide applications is the perovskite oxide, $ABO_3$. A particular application of a given perovskite compound depends on its properties which are in turn related to particle size and structural features such as doping. Lanthanum ferrite perovskite, $LaFeO_3$, offers a wide field of research due to its intriguing structural, electronic and magnetic properties. The structure, which is distorted orthorhombic deviating from the ideal cubic $ABO_3$ perovskite structure, has been widely studied [1-3]. A wide range of novel properties can be achieved through the modification of the $LaFeO_3$ structure by doping with other metal ions at the A- or B-site [1]. Noticeable modification in electrochemical, magnetic, electronic, catalytic, and conductivity properties is obtained when $La^{3+}$ is substituted by $Sr^{2+}$ in the A-site to form lanthanum strontium ferrite (LSF), $La_{1-x}Sr_xFeO_3$ and simultaneous A-site substitution of $La^{3+}$ by $Sr^{2+}$ and B-site substitution of $Fe^{3+}$ by $Co^{3+}$ to form lanthanum strontium cobalt ferrite (LSCF), $La_{1-x}Sr_xCo_yFe_{1-y}O_3$ [4]. The synthesis of LSF and LSCF in different forms such as thin films, nanopowders, nanocomposites with various properties are applicable as cathode materials for solid oxide fuel cells (SOFC), gas separation membranes, catalysts, sensors [5-7]. Solid oxide fuel cells are devices which provide renewable energy and offer many advantages over other energy sources such as high efficiency, low pollutant emissions, and the use of variety of fuels [5].

In a previous work, the structure and magnetic properties of $La_{1-x}Sr_xFeO_3$ were studied [8] and the results showed structural changes from orthorhombic to rhombohedral with increasing Sr content and increases in magnetization in the same trend similar to results obtained by other researchers [6,9,10]. The main objective of the present work is to study the effect of substituting Fe ions with Co ions on the structural and magnetic properties of one of the compositions of the $La_{1-x}Sr_xFeO_3$ system, (x =0.2) with perovskite orthorhombic structure. Since Fe and Co are present in $La_{0.8}Sr_{0.2}Co_yFe_{1-y}O_3$, the structural and magnetic properties are compared with $La_{1-x}Sr_xFeO_3$ and $La_{1-x}Sr_xCoO_3$ perovskite systems.

The structure and magnetic properties of the perovskite compounds $La_{1-x}Sr_xCoO_3$ have been reported to vary with Sr concentration amidst other physical factors like temperature, pressure and oxygen content [11]. Undoped $LaCoO_3$ is nonmagnetic with only $Co^{3+}$ ions present in the low spin state (LS: S =0; $t_{2g}^6$) at temperatures less than 100 K and becomes ferromagnetic at

temperatures between 100 K and 500 K with the $Co^{3+}$ ions having the intermediate spin state (IS: S =1; $t_{2g}^5e_g^1$). Substitution of $La^{3+}$ by $Sr^{2+}$ in the $La_{1-x}Sr_xCoO_3$ system induces the formation of $Co^{4+}$ ions to maintain electrical neutrality and there is a change from anti-ferromagnetism at low Sr concentrations (x <0.2) to ferromagnetism at higher concentrations (x ≥0.2) [11,12]. The long range ferromagnetic ordering for x≥0.2 is through the double exchange interaction. It involves the simultaneous transfer of one electron from the $Co^{3+}$ to the oxygen and another electron from the oxygen to the neighbouring $Co^{4+}$ ($Co^{3+}\Rightarrow O^{2-}\Rightarrow Co^{4+}$) with the spins maintained in the same direction [13].

A different approach of preparing $La_{0.8}Sr_{0.2}Co_yFe_{1-y}O_3$ nanopowders by thermal decomposition of the mixed metal acetylacetonate prepcursors is reported in this work. The choice of acetylacetonates as precursor is because they are less moisture sensitive, (thus rendering them less susceptible to hydrolysis), exhibit chelating effect which ensures proper mixing of the metal ions in solutions giving the required metal-metal ratios in the final mixed metal oxides [14]. In addition, the mixed metal acetylacetonates are easily prepared at low temperatures, and decomposed at moderate temperatures to give mixed metal oxide nanoparticles [15]. The structural and magnetic properties of the nanopowders are investigated to determine their suitability for various applications such as using them as electrode modifiers for the cathode materials of SOFC.

## 2. MATERIALS AND METHODS

### 2.1 Reagents

The following reagents of analytical grade were obtained from Sigma-Aldrich: $La(NO_3)_3.6H_2O$ (99%), $Sr(NO_3)_2$ (99%), $Fe(NO_3)_3.9H_2O$ (99.5%), $Co(NO_3)_2.6H_2O$ (99%), NaOH (98%), and $C_5H_8O_2$ (99.5%) from BDH respectively. They were used in this work without any further purification.

### 2.2 Preparation of $La_{0.8}Sr_{0.2}Co_yFe_{1-y}O_{3-\delta}$ (y=0, 0.2, 0.4) Nanoparticles

The different mixed metal nanopowders were prepared according to the formula $La_{0.8}Sr_{0.2}Co_yFe_{1-y}O_{3-\delta}$ {y=0.0 (LSF82), y=0.2 (LSCF8228), and y=0.4 (LSCF8246)} following a two stage procedure: firstly, the preparation of the corresponding mixed metal acetylacetonate precursors by co-precipitation [8,16] and secondly, the thermal decomposition of the precursor complexes [14,17].

#### 2.2.1 Preparation of precursors

To synthesize $La_{0.8}Sr_{0.2}Co_{0.2}Fe_{0.8}(C_5H_7O_2)_6$ with y =0.2, abbreviated LSCF8228acac, the precipitating agent, sodium acetylacetonate was first prepared by slowly adding 3 ml of acetylacetone to NaOH solution (2.9 M) while stirring and the solution maintained at 55°C for 20 minutes. Then a solution containing 1.681 g of $La(NO_3)_3.6H_2O$, 0.206 g of $Sr(NO_3)_2$, 1.569 g of $Fe(NO_3)_3.9H_2O$, and 0.282 g of $Co(NO_3)_2.6H_2O$ all dissolved inside 10 mL of double distilled water was added drop wise to the sodium acetylacetonate solution at 55°C while stirring for 30 minutes. Red precipitate of $La_{0.8}Sr_{0.2}Co_{0.2}Fe_{0.8}(C_5H_7O_2)_6$ was formed. The precipitate was allowed to cool, filtered by suction, washed three to four times with distilled water to remove by-products and unreacted reagents and dried for 5 hours at 80°C in an oven.

The synthesis of $La_{0.8}Sr_{0.2}Co_yFe_{1-y}(C_5H_7O_2)_6$ {y =0 (LSF82acac), y=0.4 (LSCF8246acac)} was each carried out by the same procedure.

#### 2.2.2 Preparation of the mixed metal nanopowders

The mixed metal oxides were formed by thermal decomposition of the mixed metal acetylacetonate complexes. Each complex was later put in an alumina crucible with lid and inserting into a preheated muffle furnace at 450°C in the presence of air for three hours. The powders formed were ground and calcined in a Nabertherm furnace at 1000°C for 6 hours at a heating and cooling rate of 5°C/min.

### 2.3 Characterization of the Mixed Metal Ferrite Precursors by Thermogravimetry

Characterization of the precursors by thermogravimetry analysis (TGA) and differential thermogravimetry analysis (DTA) was performed using a TG analyser (Model: SDT Q600 V20.9 Build 20 DSC-TGA Standard) under an inert atmosphere (nitrogen), at a heating rate of 10°C/min in an alumina crucible. TGA and DTA curves were recorded on heating from room temperature up to 900°C.

### 2.4 Characterization of the Mixed Metal Ferrites by XRD, SEM, EDS and VSM

For each composition obtained after calcinations at 1000℃, phase purity and crystal structure were determined by powder X-ray diffraction using PANalytical X'Pert PRO 1712 diffractometer. Measurements were taken in the 2θ range of 10-80°, using Cu-Kα radiation at a scan rate of 2°/min. Crystallite size was determined based on Scherrer's formula from the line broadening of the peak at around 32°. Microstructure and morphology were analyzed using a JEOL JSM-840A scanning electron microscope (SEM). The scanning electron microscope was fitted with an energy dispersive X-ray spectrometer (EDS) for the determination of the different elements present.

The magnetization measurements were performed using a vibrating sample magnetometer, VSM (model EG&G PAR 4500) at room temperature (300 K) with applied field from 0 to 15 kOe.

## 3. RESULTS AND DISCUSSION

### 3.1 Thermal Analyses (TGA-DTA)

Thermal decomposition behaviour of the precursor – LSF8228acac was studied to determine the temperature at which the mixed metal oxide was formed. The TG-DTA curves of LSCF8228acac are shown in Fig. 1. The LSCF8228acac precursor has a deep red color. Since the thrermogravimetric - differential analyses (TG-DTA) could not give qualitative information about the decomposition products; quantitative interpretation of the percentage weight loss has been done.

There are five active regions. In the first region, from 70.2℃ – 115℃, the DTA shows a sharp peak (81℃) and there is a weight loss of 7.9% which is interpreted as loss of a molecule of acetone (theoretical weight percent 7.4%). In the second region from 141.4℃ – 190℃, the DTA shows a sharp peak with two maxima (156℃, 178℃). The weight loss in the second region is 12.1% and corresponds to one acetone molecule and one acetate ion (theoretical 11.9%). The DTA shows a broad peak with two maxima (218.5°C, 258°C) in the third region from 197℃ – 339.5°C with a weight loss of 22.6% which may correspond to two acetone molecules, $CO_2$ and $H_2O$. In the fourth region, from 358℃ – 427.3℃, the DTA shows a sharp peak with two maxima (395°C, 400.9°C) and there is a weight loss of 25.6% which may correspond to two acetone, one acetate ion and $CO_2$ (theoretical 25.9%). In the fifth region from 441°C – 472°C, the DTA shows a narrow peak (458℃). The weight loss in the fifth region is 1.3% and may correspond to $H_2O$ (theoretical 2.3%).

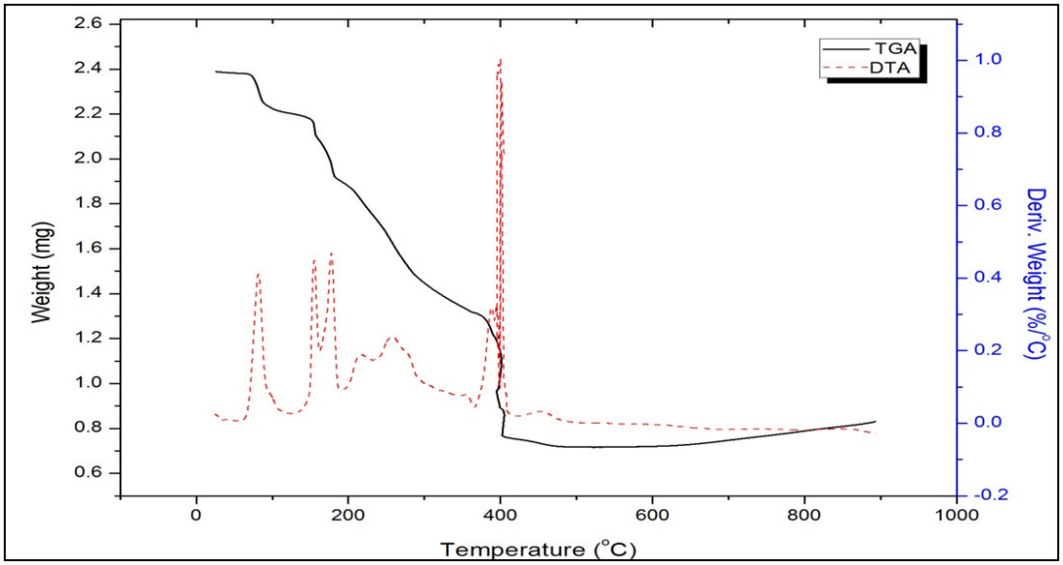


**Fig. 1. TG-DTA curves of LSCF8228acac**

The residue, which is black, is 30% (theoretical 29.9%) which can be ascribed to $La_{0.8}Sr_{0.2}Fe_{0.8}Co_{0.2}O_3$. The decomposition of lanthanum acetylacetonate [18] has been reported to evolve $CH_3CCH$, acetone, $CO_2$ and CO with $La_2O_3$ as the final residue. Decomposition of cerium acetylacetonate [19] gave acetone, acetate ion and $CO_2$ as decomposition products with $CeO_2$ as the residue. Acetone and $CO_2$ as major gaseous products from the decomposition of the acetylacetonates of Fe(III), Co(II) and Co(III) were obtained [20].

### 3.2 Structure and Particle Size (XRD)

The precursors decomposed at 450°C to form the mixed metal oxide with secondary phases. The ferrites were then heat-treated at different temperatures in the range 450 – 1000°C and x-ray diffraction patterns were taken after each calcination temperature. The Sr and Co ions incorporated completely to form a single phase perovskite only after calcination at 1000°C. Therefore, all samples were calcined at 1000°C before further analyses were performed. Fig. 2 shows the x-ray diffraction patterns of $La_{0.8}Sr_{0.2}Co_yFe_{1-y}O_3$ (y=0, 0.2, 0.4) obtained after being heat-treated at 1000°C. Crystallite sizes determined on the basis of Scherrer's formula from the line broadening of the most intense peak at around 32° are presented in Table 1.

The particles were all of nano-size with crystallite sizes ranging from 19 nm to 48 nm. The intense and broad peaks (Fig. 2) affirm that the particles are of nanosize.

**Table 1. Particle sizes of $La_{0.8}Sr_{0.2}Co_yFe_{1-y}O_3$**

| Sample | LSF82 (y=0) | LSCF8228 (y=0.2) | LSCF8246 (y=0.4) |
|---|---|---|---|
| Mean crystallite size (nm) | 48 | 36 | 19 |

Rietveld refining of the samples was done using GSAS program to determine structural and lattice parameters. Lattice parameters are presented in Table 2. The XRD pattern of the parent compound, $La_{0.8}Sr_{0.2}FeO_3$ (LSF82) possesses intense peaks (Fig. 2) which correspond to an orthorhombic structure with space group Pbnm (No 62) as indexed in JCPDS card number 13-1480 and in agreement with the literature [4,10].

An orthorhombic structure with space group Pbnm was also achieved for the sample LSCF8228 which can be indexed on the $La_{0.8}Sr_{0.2}FeO_3$ perovskite model (JCPDS card number 13-1480), similar to the literature [21]. Therefore, incorporation of a small amount of Co in the lattice maintains the structure as orthorhombic.

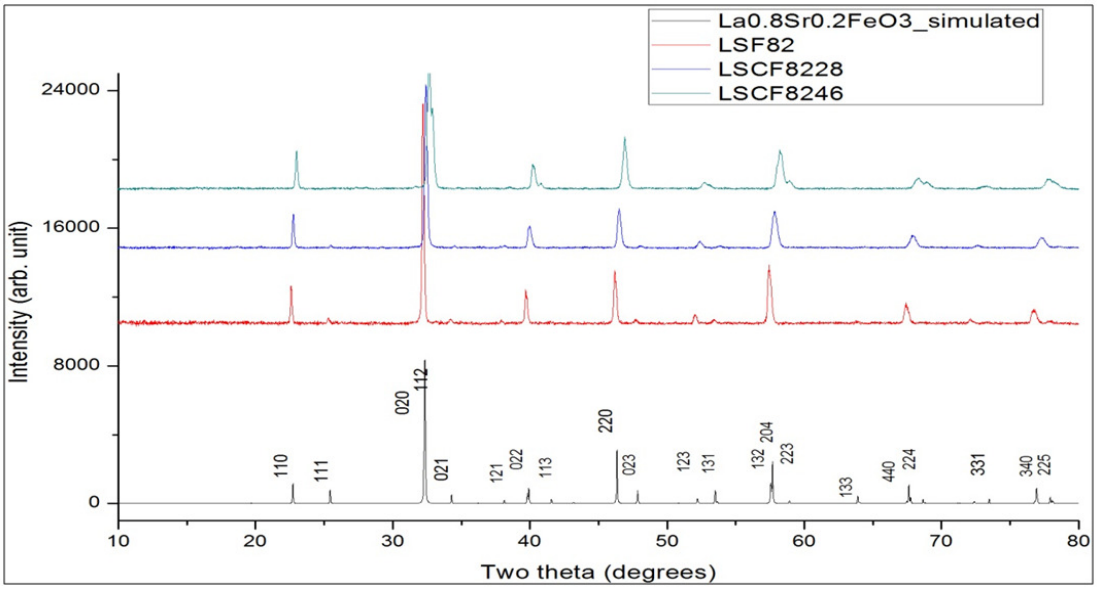


**Fig. 2. XRD patterns of $La_{0.8}Sr_{0.2}FeO_3$ simulated, LSF82, LSCF8228 and LSCF8246**

**Table 2. The results obtained from the rietveld refinement of the powder X-ray diffraction data of $La_{0.8}Sr_{0.2}Co_yFe_{1-y}O_{3-\delta}$ at room temperature. The A and B sites are fully occupied and the ratios of La/Sr and Fe/Co are fixed at the synthesis ratio**

| Sample | $La_{0.8}Sr_{0.2}FeO_{3-\delta}$ | $La_{0.8}Sr_{0.2}Co_{0.2}Fe_{0.8}O_{3-\delta}$ | $La_{0.8}Sr_{0.2}Co_{0.4}Fe_{0.6}O_{3-\delta}$ |
|---|---|---|---|
| Crystal structure | Orthorhombic | Orthorhombic | Rhombohedral |
| Space group | Pbnm | Pbnm | R-3c |
| a (Å) | 5.5491(10) | 5.5035(4) | 5.49026(21) |
| b (Å) | 5.5523(7) | 5.5317(5) | 5.49026(21) |
| c (Å) | 7.8451(11) | 7.8116(8) | 13.2828(10) |
| Vol. ($Å^3$) | 241.71(6) | 237.72(4) | 346.741(32) |
| Total O | 2.964 | 2.953 | 2.685 |
| $\delta$ | 0.036 | 0.047 | 0.315 |
| Bond angles | | | |
| Fe_O1_Fe | 169.101(2) | 162.231(2) | 165.176(0) |
| Fe_O2_Fe | 157.738(4) | 151.781(4) | |
| Co_O1_Co | | 162.231(2) | 165.176(0) |
| Co_O2_Co | | 151.781(4) | |
| Fe_O1_Co | | 162.231(2) | 165.176(0) |
| Fe_O2_Co | | 151.781(4) | |

A rhombohedral model was used for the refinement of LSCF8246 and the peaks matched better than using an orthorhombic model. Therefore, LSCF8246 shows a rhombohedral structure with space group R-3c (167). Thus, increasing Co content changed the structure from orthorhombic to rhombohedral.

The structures of $La_{0.8}Sr_{0.2}Co_yFe_{1-y}O_3$ can be better elucidated by comparing the $La_{1-x}Sr_xFeO_3$ and $La_{1-x}Sr_xCo_yFe_{1-y}O_3$ systems. $La_{1-x}Sr_xFeO_3$ ($0\leq x\leq 0.2$) shows an orthorhombic structure while $La_{1-x}Sr_xCo_yFe_{1-y}O_3$ ($0\leq x\leq 0.5$) is rhombohedral [11,22]. A low substitution (20 mol %) of $Fe^{3+}$ (ionic radius, 0.645 Å for high spin, HS) [23] by smaller $Co^{3+}$ ions (ionic radius of 0.61 Å for HS) [23] in $La_{0.8}Sr_{0.2}FeO_3$ to form $La_{0.8}Sr_{0.2}Co_{0.2}Fe_{0.8}O_3$ (LSCF8228), results in a decrease in unit cell volume (241.71 - 237.72 Å) but the orthorhombic perovskite structure is however maintained. There is also the formation of two sets of ions $Fe^{3+}$, $Fe^{4+}$ and $Co^{3+}$, $Co^{4+}$ to maintain electrical neutrality as reported in the literature [4,11,24].

Increasing the Co content changes the structure to rhombohedral at y=0.4 (LSCF8246) with a large unit cell volume (Table 2). The change in structure can be due to two reasons (i) because $Co^{4+}$ has a lower binding energy to oxygen, large amounts of cobalt substitution results in some $Fe^{4+}$ and more oxygen vacancies (Table 2) being formed. There is greater cation - cation contact, hence high repulsions and large crystal volume (ii) the presence of a large number of smaller ions ($Co^{3+}$, $Fe^{4+}$) will modify the structure so as to maintain the perovskite structure as depicted by the value of the tolerance factor, t (equation 1), which moves close to unity and fall within the rhombohedral region. A perovskite structure is cubic when *t* is approximately equal to 1, rhombohedral when *t* is between 0.96 and 1, and orthorhombic when *t* is smaller than 0.96 [25,26].

$$t = r_A + r_O/ \sqrt{2}(r_B + r_O) \quad (1)$$

Where, $r_A$, $r_B$, and $r_O$ are the relative ionic radii of the A site and B site cations and the oxygen ion respectively.

The bond angle ∠B-O1-B is the tilting angle of the octahedron and ∠B-O2-B is the rotation angle around the c axis [27]. From the refinement results in Table 2, all the B-O-B bonds are less than 180°, indicative of deviations from ideality. The bond length Co–O1 fluctuate with increasing Co doping indicating distorted $Co/FeO_6$ octahedra. The complexity of the valences of Co, Fe and the oxygen vacancies contribute to the distortion.

The La/Sr and Fe/Co ratios were fixed at the synthesis ratio during refinement. The refinement shows few oxygen vacancies in the LSF82 sample (3.6%). The oxygen vacancies increases with increasing Co content (4.7% for LSCF8228 and 31.5% for LSCF8246) since the Co ions have a smaller binding energy for oxygen than Fe ions [25]. Hence, at low Co concentration, electrical neutrality is maintained by mostly the formation of mixed transition valences and at high Co content, more oxygen vacancies are formed.

### 3.3 Morphology and Microstructure (SEM)

The SEM images of the mixed metal ferrites after calcinations at 1000℃ are shown in Fig. 3. The particle sizes are all less than 100 nm, in agreement with the XRD results. The crystallites are spherical. There is considerable agglomeration of the particles as observed by other researchers [4,28]. The SEM micrographs reveal uniformity in the texture and distribution of the particles.

### 3.4 Elemental Analysis (EDS)

Table 3 summarizes the elemental weight percentages in each composition from EDS. All the desired metallic elements are present with no other elements as indicated by the XRD curves. The metal–metal ratios are close to the required ratios. The error in each composition is within acceptable limits. Oxygen percentages are high due to detection of atmospheric oxygen by the instrument.

### 3.5 Magnetic Measurements (VSM)

Magnetic measurements were performed on the $La_{0.8}Sr_{0.2}Co_yFe_{1-y}O_{3-\delta}$ (y=0, 0.2, 0.4) nanopowders obtained after calcination at 1000℃ with a maximum applied magnetic field of 15 kOe. Fig. 4 shows the magnetization curves of LSF82 (y=0.0), LSCF8228 (y=0.2) and LSCF8246 (y=0.4) nanopowders with particle sizes of respectively 48, 36 and 19 nm measured at room temperature (300 K) by VSM.

We observe from Fig. 4 spontaneous magnetization and the appearance of hysteresis loops for all the samples when an external magnetic field is applied at room temperature. There is spontaneous ordering of the magnetic moments on the scale of microscopic domains [29], and the sum of all the domains cancel out as the unmagnetized material has no net magnetization at the origin (Fig. 4).

A magnetic hysteresis loop is formed when a magnetization curve of a ferromagnetic or ferrimagnetic material follows a different demagnetization path. Therefore the appearance of narrow hysteresis loops indicates weak ferromagnetism. The maximum field applied, 15 kOe does not saturate the magnetization as observed for all the samples. We also note a closed loop at the maximum applied field. The non-saturation of the magnetization is characteristic of anti ferromagnetic ordering of the spins in the nanoparticles.

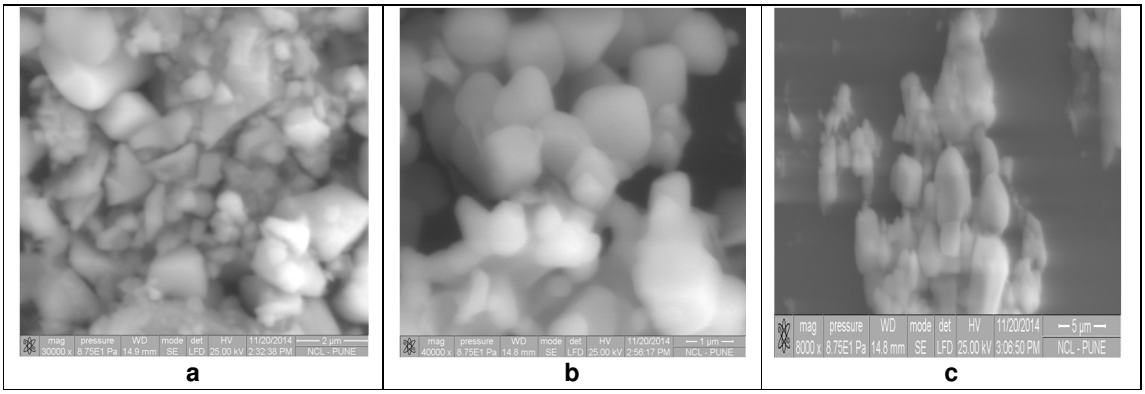


**Fig. 3. SEM micrographs of (a) LSF82, (b) LSCF8228 and (c) LSCF8246 at 2 µm**

**Table 3. Elemental analysis of LSF82, LSCF8228 and LSCF8246 from EDS analysis**

| Element | LSF82 (y =0) | | | LSCF8228 (y =0.2) | | | LSCF8246 (y =0.4) | | |
|---|---|---|---|---|---|---|---|---|---|
| | Exp. wt % | Theoretical wt % | Error % | Exp. wt % | Theoretical wt % | Error % | Exp. wt % | Theoretical wt % | Error % |
| La | 49.20 | 47.8 | 1.4 | 48.41 | 47.7 | 0.7 | 47.94 | 47.6 | 0.3 |
| Sr | 4.46 | 7.5 | 3.0 | 7.81 | 7.5 | 0.3 | 7.38 | 7.5 | 0.1 |
| Fe | 22.95 | 24.1 | 1.1 | 14.87 | 19.1 | 4.2 | 12.15 | 14.3 | 2.1 |
| Co | - | - | - | 4.87 | 5.1 | 0.2 | 7.96 | 10.1 | 2.1 |
| O | 23.39 | 20.6 | 2.8 | 24.04 | 20.6 | 3.4 | 24.57 | 20.5 | 4.0 |
| Total | 100 | 100 | | 100 | 100 | | 100 | 100 | |

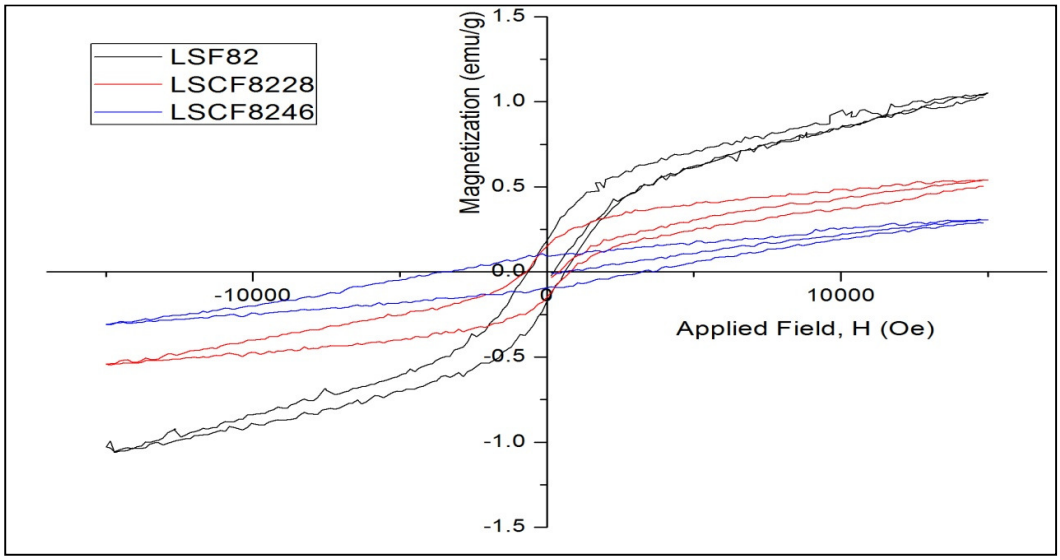


**Fig. 4. Hysteresis loops at room temperature of $La_{0.8}Sr_{0.2}Fe_{1-y}Co_yO_{3-\delta}$**

$La_{0.8}Sr_{0.2}Co_yFe_{1-y}O_{3-\delta}$ therefore exhibits both anti ferromagnetic (AFM) and weak ferromagnetic (FM) properties. The observation of anti ferromagnetism and a weak ferromagnetic component in unsubstituted and substituted $LaFeO_3$ perovskites has been well documented in the literature [1,30]. The magnetization obtained at maximum applied field and remanent magnetization (Table 4) decrease with increasing Co content. These observations can be elucidated from understanding the structures and magnetic spin interactions of the $La_{1-x}Sr_xCoO_3$ and $La_{1-x}Sr_xFeO_3$ systems.

Most studies have suggested that the spin state of $Co^{3+}$ ions in $La_{1-x}Sr_xCoO_3$ occur in three spin states: low spin ($t_{2g}^6e_g^0$, S=0), high spin ($t_{2g}^4e_g^2$, S=2) and intermediate spin, IS ($t_{2g}^5e_g^1$, S=1), but the spin state of $Co^{4+}$ ions is still an open issue, and it could be in the LS state ($t_{2g}^5e_g^0$, S=0.5), IS state ($t_{2g}^4e_g^1$, S=1.5), HS state ($t_{2g}^3e_g^2$, S=2.5) or a mixture of these states [12,24]. $La_{1-x}Sr_xCoO_3$ show long range ferromagnetic ordering for $x \geq 0.2$ through the double exchange interaction with the intermediate spin, IS ($t_{2g}^5e_g^1$, S=1) being the most abundant state for the $Co^{3+}$ ions [11].

For the $La_{1-x}Sr_xFeO_3$ system, $La_{0.8}Sr_{0.2}FeO_3$ shows a G-type anti ferromagnetic spin ordering. The anti-ferromagnetic ordering arises from the super-exchange interaction with a small ferromagnetism occurring due to the anti-parallel spins slightly canted along the c-axis as a result of the tilted $FeO_6$ octahedra. The double exchange interaction of $Fe^{3+}/Fe^{4+}$ also increases the ferromagnetic component. The Fe ions are expected to occur in the high spin state which is a stable state for oxides of iron [31].

The partial replacement of Fe by Co in $La_{0.8}Sr_{0.2}FeO_3$ implies the formation of mixed $Fe^{3+}/Fe^{4+}$ and $Co^{3+}/Co^{4+}$ couples, which result in a complex electron spin interactions. The anti-ferromagnetism in $La_{0.8}Sr_{0.2}Fe_{1-y}Co_yO_3$ system can be explained by the super exchange interaction and the ferromagnetism arises from the double exchange and spin canting. The total magnetization is the sum of the effective magnetic moments of each ion. The magnetization decreases with increasing Co substitution because the total magnetic spin contribution of Co ions ($Co^{3+}$: IS, S=1, $Co^{4+}$: HS, S =2.5) is less than that of Fe ions ($Fe^{3+}$: HS, S=2.5, $Fe^{4+}$: HS, S =2) as indicated in Fig. 4. From the literature [25], magnetic moments of 3.12 $\mu_B$ and 2.21 $\mu_B$ from neutron diffraction studies of $La_{0.8}Sr_{0.2}FeO_3$ and $La_{0.8}Sr_{0.2}Fe_{0.8}Co_{0.2}O_3$ samples respectively prepared at 1000℃ were obtained.

Table 4 shows the coercive fields with increase in y. Increasing Co substitution increases the coercive fields. Coercive field is related to particle size, magnetic anisotropy [32]. Increasing coercive fields may be due to decrease in the average particle sizes as indicated in Table 4. From the moderate coercive fields and the shape of the hysteresis loops, the compounds can be classified as soft magnetic materials [29].

**Table 4. Coercive field (Hc), magnetization (M) and remanent magnetization (Mr) of $La_{0.8}Sr_{0.2}Co_yFe_{1-y}O_{3-\delta}$ nanopowders**

| $La_{0.8}Sr_{0.2}Co_yFe_{1-y}O_3$ | Coercive field, Hc (Oe) | Maximum magnetization, M(emu/g) | Remanent magnetization Mr(emu/g) |
|---|---|---|---|
| y =0 (LSF82) | 637 | 1.06 | 0.19 |
| y =0.2 (LSCF8228) | 758 | 0.54 | 0.15 |
| y =0.4 (LSCF8246) | 3247 | 0.30 | 0.09 |

## 4. CONCLUSION

Mixed lanthanum strontium cobalt iron acetylacetonates were successfully prepared and decomposed to obtain single phase $La_{0.8}Sr_{0.2}Co_yFe_{1-y}O_{3-\delta}$ nanoparticles with structures ranging from orthorhombic to rhombohedral with increase in Co content from the XRD patterns. Microstructure analysis showed that the particles are spherical in shape, nano-sized and uniformly distributed. All samples exhibit a hysteresis loop characterized by coexisting anti ferromagnetic and weak ferromagnetic interactions. Co substitution increases the coercive force. These results show that the synthesized materials possess potential magnetic applications in data storage, logic, magnetic bubble memory and magnetic sensors.

## ACKNOWLEDGEMENTS

The authors are grateful to the Government of India and FICCI for partly financing the work through the fellowship “CV Raman International Fellowship for African Researchers” to EAN tenable at CSIR-NCL, Pune under the guidance (host scientist) of Dr. Pattayil Joy of the Division of Physical and Materials Chemistry to whom we remain indebted.

## COMPETING INTERESTS

Authors have declared that no competing interests exist.

## REFERENCES

1. Popa M, Moreno JMC. Lanthanum ferrite ferromagnetic nanocrystallites by a polymeric precursor route. Journal of Alloys and Compounds. 2011;509:4108–4116.
2. Sorescu M, Xu T, Hannan A. Initial stage growth mechanism of $LaFeO_3$ perovskite through magnetomechanical ball-milling of lanthanum and iron oxides. American Journal of Materials Science. 2011;1(1): 57-66.
3. Sivakumar M, Gedanken A, Zhong W, Jiang YH, Du YW, Brukental I, Bhattacharya D, Yeshurunc Y, Nowik I. Sonochemical synthesis of nanocrystalline $LaFeO_3$. J Mater. Chem. 2004;14:764–769.
4. Ulrich FV, Josef S, Joerg R, Christian S, Peter H. B-site substituted lanthanum strontium ferrites as electrode materials for electrochemical applications. Pure Appl Chem. 2008;80(11):2543–2552.
DOI: 10.1351/pac200880112543
5. Baharuddin NA, Rahman HA, Muchtar A, Sulong AB, Abdullah H. Development of lanthanum strontium cobalt ferrite composite cathodes for intermediate- to low-temperature solid oxide fuel cells. J Zhejiang Univ-Sci A (Appl Phys & Eng). 2013;14(1):11-24.
6. Li S, Jin W, Huang P, Xu N, Shi J, Lin YS. Tubular lanthanum cobaltite perovskite type for oxygen permeation. Journal of Membrane Science. 2000;166:51–61.
7. Macedo DA, Moisés RC, Beatriz C, Carlos AP, Dulce MA Melo, Rubens MN, Antonio EM. Lanthanum manganite and cobaltite-based composite cathodes for SOFCs, 2012. International Conference on Power and Energy Systems Lecture Notes in Information Technology. 2012;13.
8. Nforna EA, Ghogomu JN, Joy PA, Lambi JN. Structure and magnetic properties of lanthanum strontium ferrite nanopowders synthesized by thermal decomposition of mixed metal acetylacetonates. IJERT. 2015;4(7):907-914.
ISSN: 2278-0181
9. Patrakeev MV, Bahteeva JA, Mitberg EB, Leonidov IA, Kozhevnikov VL, Poeppelmeier KR. Electron/hole and ion transport in $La_{1-x}Sr_xFeO_{3-\delta}$. Journal of Solid State Chemistry. 2003;172:219-231.

10. Jiangong L, Xinli K, Yong Q, Haiying H. Microstructure and magnetic properties of $La_{1—x}Sr_xFeO_3$ nanoparticles. Phys. Stat. Sol. 2002(a);191(1):255–259.
11. Xiangfan X, Lizhen J, Jingqin S, Zhangjian C, Zhuan X. Relationship between Spin State of Co ions and thermopower in $La_{1-x}Sr_xCoO_3$. Physics Letters A. 2006;351: 431–434.
12. Pietosa J, Wisniewski A, Puzniaka R, Kolesnik S, Majjiga M, Dabrowski B. Influence of pressure on magnetic properties of $La_{1-x}Sr_xCoO_{3-\delta}$ (x=0.5, 0.67, 1). Acta Physica Polonica A. 2006; 109(4-5):527-532.
13. Farhoudi MM. Studies of structures, transport and magnetic properties od doped novel three dimensional perovskite compounds. Ph.D. Dissertation. University of Wollongong; 2009.
14. Schwartz RW, Schneller T, Waser R. Chemical solution deposition of electronic oxide films. C. R. Chimie. 2004;7:433-461.
15. Lieberman CM, Navulla A, Zhang H, Filatov AS, Dikarev EV. Mixed-ligand approach to design of heterometallic single-source precursors with discrete molecular structure. Inorg Chem. 2014; 53:4733-4738.
16. Charles RG, Pawlikowski MA. Comparative heat stabilities of some metal acetylacetonate chelates. 1958;62:440-444.
17. Pal B, Sharon M. Preparation of iron oxide thin film by metal organic deposition from Fe III -acetylacetonate: A study of photocatalytic properties. Thin Solid Films. 2000;379:83-88.
18. Hussein GAM, Ismail HM. Characterization of lanthanum oxide formed as a final decomposition product of lanthanum acetylacetonate: Thermoanalytical, spectroscopic and microscopic studies. Powder Technology. 1995;84:185-190.
19. Ristoiu T, Ciontea L, Suciu RC, Petrisor Jr T, Gabor MS, Thalmayer Gy, Petrisor T. Thermal decomposition study by DTA-TG-MS of cerium[III] acetylacetonate used as ceria thin film precursor. Journal of Optoelectronics and Advanced Materials. 2008;10(9):2223–2227.
20. Vokhoene J, Charlesand RG, Hicka WM. Thermal decomposition of metal acetylacetonates mass spectrometer studies. 1958;62:1098-1101.
21. Ghosh S, Dasgupta S. Synthesis, characterization and properties of nanocrystalline perovskite cathode materials. Materials Science-Poland. 2010; 28(2):427-438.
22. Efimov V, Efimova E, Karpinsky D, Kochubey DI, Kriventsov V, Kuzmin A, Molodtsov S, Sikolenko V, Tiutiunnikov S, Troyanchuk IO, Shmakov AN, Vyalikh D. XAFS and neutron diffraction study of the $La_{1-x}Sr_xCoO_3$. Phys. Stat. Sol. 2007c; 4(3):805–808.
DOI: 10.1002/pssc.200673874
23. Shannon RD. Revised effective Ionic radii and systematic studies of interatomie distances in halides and chaleogenides. Acta Crystallographica. 1976;A32:751-767.
24. Sundarum N, Jiang Y, Anderson IE, Belanger DP, Booth CH, Bridges F, Mitchell JF, Proffen Th, Zheng H. Local structure of $La_{1-x}Sr_xCoO_3$ determined from EXAFS and neutron pair distribution function studies. PRL. 2009;102:026401.
25. Qingsheng C. Neutron diffraction studies on $ABO_3$ (A=La, Sr, B=Fe, Co, Ni, Cu, Mn, Ti). Perovskite used in solid oxide fuel cell (SOFC) and double perovskite, $Ba_2YRu_{0.8}Cu_{0.15}O_6$ superconductor. Ph.D. Dissertation. University of Missouri-Columbia. USA; 2009.
26. John Irvine TS, Paul Connor (editors). Solid oxide fuels cells: Facts and figures. Springer-Verlag London; 2013.
DOI: 10.1007/978-1-4471-4456-4
27. Yi-Jie G, Zhi-Ning Y, Yun-Bo C, Hong-Quan L, Hui-Kang W, Lin C, Meng W, Lin-Li Z, Xiao-Wen H, Xiu-Bo L, Wen-Ge W, Cheng L, Yong H, Zhen G, Zu-Wang H. Structural analysis of multiphase $La_{1-x}Sr_xCo_{1-x}Fe_xO_{3-\delta}$. Advanced Materials Research. 2011;177:74-77.
28. Bayraktar D, Clemens F, Diethelm S, Graule T, Herle JV, Holtappels P. Production and properties of substituted $LaFeO_3$-perovskite tubular membranes for partial oxidation of methane to syngas. Journal of the European Ceramic Society. 2007;27:2455–246.
29. Coey JMD. Magnetism and magnetic materials. Cambridge University Press. New York; 2009.
ISBN-13 978-0-511-67743-4
30. Sora IN, Caronna T, Fontana F, Ferna´ndez CJ, Caneschi A, Green M. Crystal structures and magnetic properties of strontium and copper doped lanthanum ferrites. Journal of Solid State Chemistry. 2012;191:33–39.

31. Shruba G, Talgat I, Artem EM, Deanna A, Nina O. Structural characterization combined with the first principles simulations of barium/strontium cobaltite/ ferrite as promising material for solid oxide fuel cells cathodes and high-temperature oxygen permeation membranes. Applied Materials and Interfaces. 2009;1(7):1512-1519.
32. Shein IR, Shein KI, Kozhevnikov VL, Ivanovskii AL. Band structure and the magnetic and elastic properties of $SrFeO_3$ and $LaFeO_3$ perovskites. Phys. Solid State. 2005;47:2082.



*Peer-review history:*
*The peer review history for this paper can be accessed here:*
*http://sciencedomain.org/review-history/15612*